Astrometric Detection of "Cold Jupiters"

Rob Olling

USNO/USRA, Washington, DC

ABSTRACT

I present a semi-analytic method to estimate the number of extra-solar giant planets (ESGPs) that can be detected at a given confidence level (N_σ) by future astrometric missions. Specifically, I present the cases for OBSS-A, GAIA and OBSS-B. As expected, the number of detected ESGPs is a strong function of astrometric accuracy. I present a prescription that allows for the determination of the relative numbers of ESGPs as a function of mission parameters.

Missions such as GAIA or OBSS-A can discover roughly 28,300 systems at the $N_\sigma \geq 5$ level and "determine orbits" ($N_\sigma \geq 15$) for 3,200 systems. Although the confidence level is only three times larger for orbit determination, only one in nine of the detected systems will have $N_\sigma \geq 15$.

For OBSS-B, with 2.2 times worse astrometry, the numbers are 6,100 at the $N_\sigma = 5$ level, and 510 at the $N\sigma = 15$ level, or 4.6 and 6.2 times smaller numbers than for OBSS-A/GAIA.

Independent of mission specifics, most ESGPs will be detected around M-type stars, if the planet frequency is independent of stellar mass: 54% [77%] for OBSS-A/GAIA and 70% [86%] for OBSS-B at the 5-σ [15-σ] level.

Independent of the parameters of the planetary system, most detectable ESGPs have periods of about 0.82 times the mission duration.

As might be expected, most ESGPs will be detected at bright magnitudes: brighter than $V \approx 15$ [$V \approx 13$] for detection at the 5-σ [15-σ] level for K- and earlier type stars.

1. Introduction

Several distance limits play a role in figuring out how many extra-solar giant planets (ESGPs) can be detected by an astrometric mission. I present a self-consistent semi-analytical framework that describes the chances of detection for all orbital periods and mass ratios.

The results are presented in six figures and six tables for the OBSS-A/GAIA and OBSS-B mission parameters. The former missions are assumed to have mission-end astrometric accuracies of 10 μas, while OBSS-B would reach 22 μas.

Since the number of detectable ESGPs (N_{ESGP}) is proportional to the number of parent stars, N_{ESGP} will be proportional to the volume that is "accessible" by the observational capabilities of a given astrometric mission. The better the astrometric accuracy, the more distant stars can be probed for planetary systems. Because the volume is roughly proportional to the third power of the distance, N_{ESGP} will be a strong function of the limiting distance (astrometric accuracy).

I discuss the various distance limits in section 2. In section 3, I present an analytical framework that allows for the determination of the limiting distance for given parameters of the planetary system and the mission parameters. Subsections 3.2 and 3.3 present the ESGP probability density distribution from Tabachnick & Tremaine (2002) and the procedure to estimate the actual number of expected ESGPs, respectively. In section 4, I present a methodology that allows one to estimate the relative performance of missions with differing levels of performance.

2. Distance Limits

2.1. Photometric Distance

Given a stellar type (mass) with a given absolute luminosity one can "see" the star to the following distance:

$$d_{MV}(V) \quad = \quad 10^{(+0.2*(V-M_V+5))} \ [pc] \tag{1}$$

where V is the apparent magnitude and M_V the absolute magnitude.

Given the presence of a floor level for astrometric accuracy of δ_{X0} for all apparent magnitude brighter than V_f, it makes sense to choose as a limiting magnitude the faintest magnitude that yields astrometric uncertainty of $\delta_{X0,f}$. For an OBSS-A or GAIA incarnation, $\delta_{X0,f} \sim 10$ μas. However, the floor magnitude depends on spectral type because: 1) red stars have more photons per unit energy than blue stars, 2) more photons result in better accuracy. For A5V, F5V, G5V, K5V and M2V stars, these floor magnitudes are: V_f=14.0, 14.10, 14.20, 14.44 and 14.75 mag which correspond to limiting distances of 2630, 1319, 661, 256 and 89 pc, respectively[1]. However, as I will show below, it turns out that these distance limits may be substantially relaxed for the later type stars.

---

[1]These and other auxiliary stellar parameters are also listed in table 5.

Understanding the planet-detection capabilities of a given mission is most easily accomplished by looking at circular orbits. For such systems, the geometry is straight forward so that analytical expressions can be easily derived. While these analytical expressions are known to be incorrect, they are a reasonable first order estimate. For systems with elliptical orbits, similar effects occur that change the details of the predictions, but not the order of magnitude of the effect. The number of observable ESGPs depends on the *volume* in which the astrometry is sensitive enough to pick up the wobble induced by the ESGP. The volume being proportional to the cube of the distance, the number counts are reliable to within a factor of Δd^3, where Δd is error on the distance.

2.2. Astrometry of Binary Systems

With these limitations in mind, I start with the standard expression of the semi-major axis of a binary system:

$$a = (a_1 + a_2) = \Pi \left[(M_1 + M_2) P_{yr}^2 \right]^{1/3} = \frac{1000}{d} \left(M_T P_{yr}^2 \right)^{1/3} \qquad \text{[mas]} \qquad (2)$$

$$a_2 = a \frac{M_1}{M_T} \quad \text{and} \qquad a_1 = a \frac{M_2}{M_T} = \frac{1000}{d} \left(\frac{P_{yr}}{M_T} \right)^{2/3} M_2 \qquad (3)$$

and

$$a_{1,PL} = \frac{1000}{d} \left(\frac{P_{yr}}{M_T} \right)^{2/3} M_{PL} \qquad \text{[}\mu\text{as]} \qquad (4)$$

Here a, a_1, a_2 and the parallax (Π) are expressed in in the same unit (e.g., mas), while d is the distance in units of pc. The sum of the masses (M_T), as well as the primary (M_1) and secondary (M_2) are in units of solar masses, and the orbital period (P_{yr}) is in years. The semi-major axes of the orbits of the primary and the secondary are a_1 and a_2, respectively. The semi-major axis induced by a planetary mass (M_{PL}, expressed in Jupiter masses) is of order one-thousand times smaller, so that the units of eqn. (4)] are 1000 times smaller [i.e., μas]. For circular motion, the sky positions as a function of time is given by:

$$x_{1,2} = a_{1,2} \cos (2\pi \, t/P + \phi) \qquad (5)$$

$$y_{1,2} = a_{1,2} \sin (2\pi \, t/P + \phi) \cos i \qquad (6)$$

where ϕ is the phase, and where I have chosen the orientation of the coordinate system such that the y axis is foreshortened by the $\cos i$-factor due to the inclination (i). To analyze and parameterize the effects of "binary" motion, I use three regimes of t/P, where the companion may be a star, brown dwarf of planet. First, for mission durations (T_M) much longer than the orbital period, the photocenter orbits many times around the center of mass during the mission. The distance limit I infer from this criterion is the "photocenter distance," which I

work out in §§ 2.3 in more detail. In this case, so as to be able to recognize the system as being binary, one needs to resolve the semi-major axis of the (photocentric) orbit.

In the second regime, the orbital period is much larger than the mission time so that the orbit can be reasonably well approximated as a parabola [i.e., $x(t) = x_0 + v_x t + \frac{1}{2}\dot{v}_x t^2$, where x_0 is the position at time $t = 0$, and the velocity v_x and acceleration $\dot{v}_x$ are essentially constant during the mission duration]. Traditionally, this is the method employed to discover "binaries" (e.g., Kaplan & Makarov, 2003, AN, 324, 5, 419), and I have used this method in my previous reports. However, this approximation is less relevant because this approximation is only valid for periods much longer than the mission duration, while I expect (see below) that most detected ESGPs will have periods similar to T_M. Therefore, I have investigated the intermediate regime and use the results in this memo.

The third regime is intermediate between the two cases, and is a little harder to treat, but nevertheless doable. The principle of the method is to describe the stellar positions by a constant proper motion model (neglecting paralactic motion). The quality of the fit is then a measure how well the observed motion can be represented by the linear model. Rather than quantifying the quality of the fit by χ^2, I choose as a metric the rms-size of the residuals after the linear model has been subtracted from the observations. A star can then be flagged as a possible binary when the inferred position errors are substantially larger than those of its peers of similar apparent magnitude and number of observations.

The implementation of this method is based on Monte-Carlo simulations of the orbits, and works as follows: 1) For a large number of $\tau = T_M/P$ values I randomly pick an orbital phase ϕ and inclination i, 2) I then select several 100 "observing times" between $t = 0$ and $t = t_M$ and calculate the $x(t)$ and $y(t)$ coordinates, with the y positions foreshortened due to inclination, 3) For each of the coordinates separately, I fit a linear relation to the time-coordinate data to determine the proper motions along the two directions, 4) I then rotate the coordinate system such that the spatial coordinate (z) coincides with the direction of the average orbital motion [$x = z\cos\theta$, and $\cos\theta = v_x/\sqrt{v_x^2 + v_y^2}$], 5) if $v_x > v_y$, I project the x coordinates onto the z-axis, otherwise I use the projection of the y-axis onto the z-axis to generate a $[t, z(t)]$ data set, 6) I fit a linear relation to the $z(t)$ data and subtract this linear relation of the $z(t)$ data values, and finally, 7) the metric that is indicative of significant binary motion is the RMS (σ_z) of the difference between the "observed" and fitted $z(t)$ points.

Although this metric is hard to describe analytically, it is easy to implement numerically. Also, it has the advantage that it "works" in the very short period, the very long period regime as well as for intermediate periods. However, this metric is not equivalent to orbit fitting, rather it is an indication as to whether the residuals with respect to a linear-motion

model are indicative of binarity. Unfortunately, σ_z is not a simple function but it can be approximated to reasonable accuracy [$\pm 0.2\%$ (2.6% peak-to-peak)] as:

$$\zeta(\tau) \;\equiv\; \frac{\sigma_z(\tau)}{a_i} \;\approx\; \gamma \times \left[1 - e^{-\frac{1}{2}(\tau/0.67)^2)}\right] \qquad\qquad\qquad \text{for } \tau \leq 0.75 \quad (7)$$

$$\zeta(\tau) \;\equiv\; \frac{\sigma_z(\tau)}{a_i} \;\approx\; \gamma \times \left[1 - e^{-\frac{1}{2}[(\tau+2.74)/1.90]^2)}\right] + 0.28\frac{\cos(1.30\,\pi\,\tau)}{1+\tau^4} \quad \text{for } \tau > 0.75 \quad (8)$$

$$\text{with}\,\gamma \;\approx\; 0.74644 \qquad\qquad\qquad\qquad\qquad\qquad\qquad\qquad\qquad\qquad (9)$$

where I have not attempted to make $\zeta(\tau)$ continuous[2] at $\tau = 0.75$. Although $\zeta(\tau)$ looks complicated, its form is basically "a constant minus a Gaussian centered on $\tau = 0$," with some wiggles for $0.5 \lesssim \tau \lesssim 5$.

2.3. $T_M >> P$: "Photocenter Distance"

Evaluating eqn. (8) in the "photocenter distance" regime with $T_M/P >> 1$, it follows that the average displacement due to binarity equals $0.746\,a_1$. Solving the motion of the primary in eqn (4) for the distance, and requiring that the semi-major axis equals N_σ times the astrometric error (σ), I derive the "photocenter distance" (d_{PHC}). This photocenter distance is the distance out to which the semi-major axis of the photocentric orbit is resolved at the N_σ level.

$$d_{PHC} \;\sim\; 7.46 \times \left(\frac{P_{yr}}{M_{Star} + M_{PL;S}}\right)^{2/3} \times M_{PL} \times \frac{10}{N_\sigma} \times \frac{10\,\mu\text{as}}{\delta_{X0,f}} \quad [pc] \qquad (10)$$

with M_{Star} the stellar mass, $M_{PL;S}$ [M_{PL}] the mass of the planet in units of the Sun's mass [in Jupiter masses (M_J)], and where I have used the average foreshortening due to inclination. Equation (10) shows that the following properties allow for the detection of ESGPs at larger distances: 1) longer-period systems, 2) stars of smaller mass, 3) planets of higher mass, 4) relaxing the detection criterion, and 5) better astrometric accuracy.

A larger value for d_{PHC} means that more ESGPs will be detected since the number of stars increases roughly as the third power of distance. Thus, for example, all other things being equal, a worsening of astrometric accuracy by a factor of two reduces the number of detectable planets by a huge factor of 2^3=8. For orbit determination, similar arguments hold.

---

[2]Numerically, I solve the discontinuity by computing the weighted average of the left- and right-hand parts in the transition region ($\tau \in [0.65, 0.85]$), where the weights vary linearly between three and zero.

Equation (10) above is valid in the region where the astrometric accuracy is independent of apparent magnitude. At fainter magnitudes, the astrometric accuracy is a function of magnitude. Assuming photon statistics, I get: $\delta_{X0}(V) = \delta_{X0,f} \, 10^{0.2\,(V-V_f)}$, where $V = M_V + 5\log d - 5$. Note that $\delta_{X0}(V)$ *must* exceed $\delta_{X0,f}$, so that one needs: $M_V + 5\log d - 5 - V_f \geq 0$, or $\log d \geq (V_f + 5 - M_V)/5$. The result is:

$$d_{PHC,MV} = \sqrt{d_{PHC}\, d_{tr}} \propto \sqrt{1/\delta_{X0,f}} \qquad \text{for } d_{tr} \leq d_{PHC} \leq d_{f+} \qquad (11)$$

with

$$d_{tr} = 10^{(V_f+5\ \ -M_V)/5} \qquad\qquad (12)$$

$$d_{f+} = 10^{(V_f+5+4-M_V)/5} \sim 6.3\, d_{tr} \qquad\qquad (13)$$

where the distance is in units of parsec. Also, remember that V_f depends on spectral type. Note that with these relations, $d_{PHC,MV}$ equals d_{PHC} at the transition distance d_{tr}. Here I also assume that the astrometric accuracy follows photon-statistics over a range of 4 magnitudes (to $V_{f+} = V_f + 4 = 18$ [18.75] for AV [MV] stars for OBSS-A & GAIA), and that fainter stars will not be used for planet detection. This additional criterion can be relaxed if the mission design allows so, if not, the distance is limited to d_{f+} or about 6.3 times d_{tr}. I will use the symbol $\tilde{d}_{PHC}$ to indicate either d_{PHC} or $d_{PHC,MV}$, whichever is appropriate.

2.4. $T_M << P$: "Curvature Distance"

Rather than fitting a parabola to the astrometric data, I apply the procedure appropriate for the intermediate regime to the long-period case as well. In this case, T_M/P is much smaller than unity so that equation (7) applies. The requirement that the binarity-induced residual RMS is detectable reduces to:

$$N_\sigma \delta_{X0} \leq a_1\, \zeta(\tau) \qquad\qquad (14)$$

$$\approx \tfrac{1}{2}\frac{\gamma}{0.67^2}\, a_1 \left(\frac{T_M}{P}\right)^2 \approx 0.83\, a_1 \left(\frac{T_M}{P}\right)^2 \qquad\qquad (15)$$

Substituting eqn (4) for a_1, and solving for the curvature distance I get:

$$d_C = 8.3\, T_M^2\, M_{PL} \left(\frac{1}{P_{yr}^2\, M_{tot}}\right)^{2/3} \times \frac{10}{N_\sigma} \times \frac{10\,\mu\mathrm{as}}{\delta_{X0,f}} \qquad\qquad (16)$$

$$d_{C,MV} = \sqrt{d_C\, d_{tr}} \qquad\qquad \text{for } d_{tr} \leq d_{PHC} \leq d_{f+} \quad [pc] \qquad (17)$$

with T_M in years. This curvature distance is the distance out to which the curved orbit of the photocentric orbit is still recognizable as being non-linear at the N_σ level. To arrive at

eqn. (17), I have applied the formalism leading to eqn. (11) above. Note that the transition distance, where d_{MV} takes over from d, is identical for the photocenter and curvature distances. I will use the symbol $\tilde{d}_C$ to indicate either d_C or $d_{C,MV}$, whichever is appropriate.

Obviously –and contrary to the photocenter distance– the curvature distance *decreases* with orbital period. After all, for orbital periods much exceeding the mission length, the star's motion is essentially rectilinear.

2.5. General Case

The solution of the general case [eqn. (14)] is just as straightforward:

$$N_\sigma \delta_{X0} \ \leq \ \zeta(\tau)\, a_1 \ = \ \frac{1000}{d} \left(\frac{P}{M_{tot}}\right)^{2/3} M_{PL}\ \zeta(\tau) \qquad [\mu as] \qquad (18)$$

$$d_{PHC,C} \ = \ 10.0 \left(\frac{P}{M_{tot}}\right)^{2/3} M_{PL}\ \zeta(\tau) \times \frac{10}{N_\sigma} \times \frac{10\,\mu as}{\delta_{X0,f}} \qquad (19)$$

$$d_{PHC,C,MV} \ = \ \sqrt{d_{PHC,C}\, d_{tr}} \qquad \text{for } d_{tr} \leq d_{PHC} \leq d_{f+} \qquad (20)$$

where the units for distance are parsec.

3. Synergy

Since the general case is too complicated to gain much insight, I now concentrate on the two limiting cases and extrapolate into the intermediate period regime. Requiring that a star lies within the photocenter distance *and* the curvature distance leads to a maximum distance (d_{max}) out to which an ESGP can be recognized by it's astrometric signature. This maximum distance corresponds to the intersection of the $\tilde{d}_{PHC}$ and $\tilde{d}_C$ curves, and occurs at a unique orbital period, $\tilde{P}$, given by:

$$\tilde{P}^{aprox} \ \equiv \ P^{aprox}(\tilde{d}_{PHC} = \tilde{d}_C) \ = \ P^{\tilde{aprox}}(d_{max}) \ = \ \sqrt{\frac{8.3}{7.46}} \times T_M \qquad (21)$$
$$\sim \ 1.05\, T_M$$

This period only depends on the mission length. Note that its value corresponds to $\tau = 0.95$ and lies hence in the long-period regime. In this case, the maximum distance can be found by differentiating eqn. (8) with respect to τ and finding the extremum. This value of τ_{max} yields $\zeta(\tau_{max})$ and $\tilde{P}$ for a given mission duration and yields d_{max} with eqns. (19) and (20). Numerically, I find that the exact period is about 27% smaller than approximate value:

$$\tilde{P}^{exact} \ \sim \ 0.823\, T_M \qquad (22)$$

For this case, where the maximal distance out to which an ESGP is detectable is given by:

$$d_{max} \sim 6.55 \left(\frac{T_M}{M_{tot}} \right)^{2/3} \times M_{PL} \times \frac{10}{N_\sigma} \times \frac{10\,\mu as}{\delta_{X0,f}} \tag{23}$$

$$d_{max,MV} = \sqrt{d_{max}\, d_{tr}} \qquad \text{for } d_{tr} \leq d_{PHC} \leq d_{f+} \tag{24}$$

and

$$d_{max}^{aprox} \approx 1.18\, d_{max} \qquad \text{and} \qquad d_{max,MV}^{aprox} \approx \sqrt{d_{max}^{aprox}\, d_{tr}} \tag{25}$$

and depends on the mission parameters as well as those of the binary system. The relevant scaling relations are rather obvious here: The maximum distance increases as: 1) the astrometry improves, 2) the planetary mass increases, 3) as the mission duration increases, 4) as the stellar mass decreases, and 5) if the detection threshold is lowered.
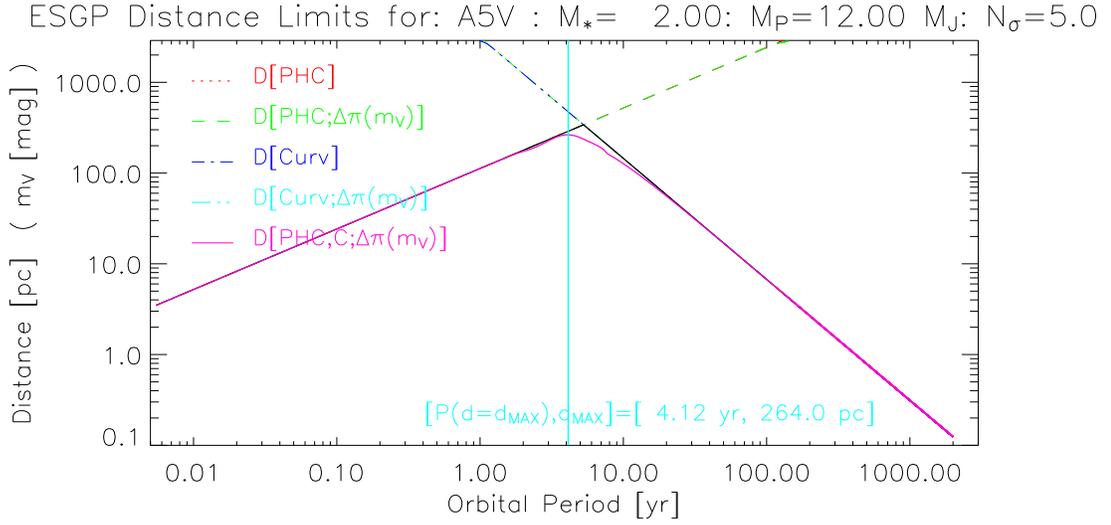
In figure 1, I plot the various distances and some derived quantifies for an A5V primary, a 12-Jupiter planet and a "detection" criterion of $N_\sigma=5$. In the top panel, I plot all distance limits ($\tilde{d}_{PHC}$, $\tilde{d}_C$ and $\tilde{d}_{PHC,C}$). Also plotted is the orbital period that corresponds to the maximum distance out to which the ESGP can be detected is indicated by the vertical (cyan) line, which is determined numerically from the exact distance relation [eqns. (19) and (20)]. If a given ESGP is to be detected, it needs to be closer than the $\tilde{d}_{PHC,C}$ which is indicated by the thick, curved (purple) line. This period-distance relation determines how much volume (full, cyan curve in bottom panel) is "accessible" to this particular primary-secondary combination (see below). Also plotted in the bottom panel are the ESGP probability density function (PDF, dashed, purple, line), the number of detectable ESGPs [N_{ESGP} (dashed-dotted, orange, line)], and the apparent magnitude (dashed-triple dotted [blue] curve). The number of expected ESGPs equals simply the product of the accessible volume, times the stellar density, times the probability that a star has an ESGP. I discuss each term in the subsections below.

3.1. Accessible Volume

The number of stars surveyed that are amenable to the detection of a given planetary mass orbiting a star of known mass is then simply equal to the the local volume density of the star (ρ_*) times the accessible volume. Here I use the stellar density in the mid-plane of the Galaxy. In the bottom panels of figures 1 and 2, I also present the accessible volume (drawn cyan), computed as:

$$Vol_{acc} = 2\pi h_z \times \left[2 \left(e^{-d/h_z} - 1 \right) h_z^2 + d(2h_z e^{-d/h_z} + d) \right] , \tag{26}$$

with h_z the vertical scale-height of the stellar population. Here Vol_{acc} is the volume that, if multiplied by ρ_* yields the total number of stars out to d. This relation is exact for a a
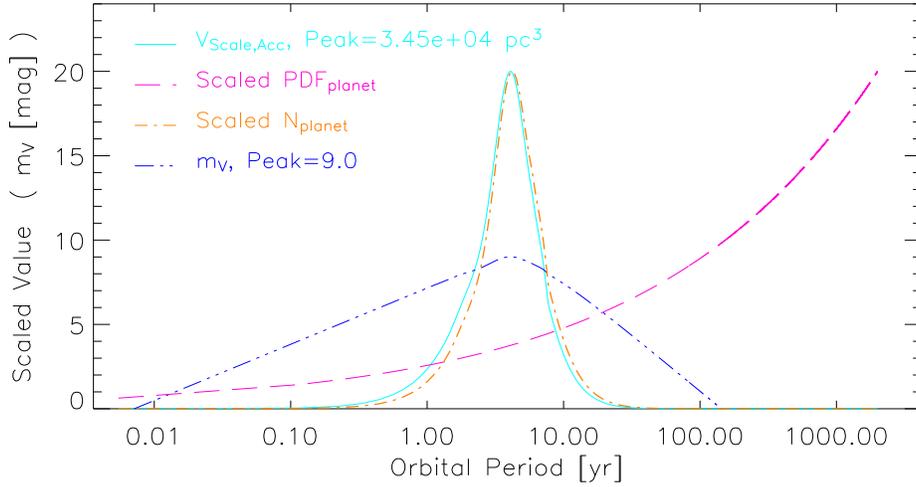
Fig. 1.— This figure presents an analysis of detectability of ESGPs by OBSS-A/GAIA for the case that the primary is an A5 main-sequence star, and the secondary a 12-Jupiter mass planet. *Top panel:* d_{PHC} (red dotted line) and d_C (dashed-dotted blue line) as a function of orbital period. The dashed line (green) is the magnitude-corrected distance $d_{PHC,MV}$, and the dashed-triple-dotted line (cyan) represents $d_{C,MV}$. The intersection of $d_{PHC,MV}$ and $d_{C,MV}$ yields $\tilde{P}$ and the maximum distance d_{MAX} out to which the ESGP can be resolved according to eqn. (24). The exact period and d_{max} are indicated by the vertical line (cyan). The thick (black) line is the $d_{max}(P)$ relation based on the two limiting case, the thick curved (purple) is the exact relation based on eqn. (19). *Bottom Panel:* In the bottom panel, the apparent magnitude (blue dashed-triple-dotted line), the scaled ESGP probability (dashed purple line), the scaled accessible volume (drawn cyan line) and the scaled number of planets (dashed-dotted orange line) are plotted. The ESGP PDF plotted is integrated over a ±1% range in mass *and* period.

"plane-parallel sheet" with constant density in the plane, and an exponential vertical density distribution. For distances not too far from the Sun, this approximation is reasonable. The following expression for the accessible volume is accurate to $\pm 5\%$ (peak-to-peak; 0.25% RMS) or so:

$$Vol_{acc} \sim \pi h_z^3 \left(\frac{d}{h_z}\right)^\kappa \tag{27}$$

$$\text{with}: \kappa \sim 2.64 + \frac{X}{10^4}(-1630 + X(-93.5 + X(64.5 + X(2.16 - 1.30X)))) \tag{28}$$

$$\text{and}: X = \ln\frac{d}{h_z} . \tag{29}$$

Equation (27) can be inverted iteratively to yield $d(Vol_{acc})$, with $\kappa = 2.5$ as a starting value. Note that the exponent κ ranges from 2.93 to 2.64 to 2.15 for (d/h_z) near zero, equal to unity and approaching infinity, respectively.

3.2. ESGP Probability Density Distribution

I use the Probability Density Distribution (PDF) derived by Tabachnick & Tremaine (2002, MNRAS, 335, 151) to estimate the actual number of detected ESGPs, as a function of planetary mass and period. Note that they determined their PDF for planets with masses between 0.5 and 12 M_J and periods up to 10 years. The basic features of this PDF are that the probability of having a planet increases with planetary mass, and that the PDF decreases with orbital period. Integrating this PDF between 0.1 and 10 M_J and period of 2 days and 10 years yields an overall probability of just about 8%. For convenience, I repeat their PDF here:

$$Prob_{PL}(M, P) \sim \frac{C}{MP}\left(\frac{M_0}{M}\right)^\alpha \left(\frac{P_0}{P}\right)^\beta \tag{30}$$

and

$$N_{PL}(M_1, M_2, P_1, P_2) \sim \frac{C}{\alpha\beta}\left[\left\{\left(\frac{M_0}{M_1}\right)^\alpha - \left(\frac{M_0}{M_2}\right)^\alpha\right\} \times \left\{\left(\frac{P_0}{P_1}\right)^\beta - \left(\frac{P_0}{P_2}\right)^\beta\right\}\right] \tag{31}$$

with :

$$C \sim 1.904\,10^{-3} \quad \alpha \sim 0.11 \quad \beta \sim -0.27$$
$$M_0 = 1.5 \qquad\qquad [M_J]$$
$$P_0 = 90.0 \qquad\qquad [days]$$

where the periods (P, P_0, P_1, P_2) are measured in days, the masses (M, M_0, M_1, M_2) in Jupiter masses, and where the PDF is integrated over the following ranges: $M_1 \le M_{PL} \le M_2$ and
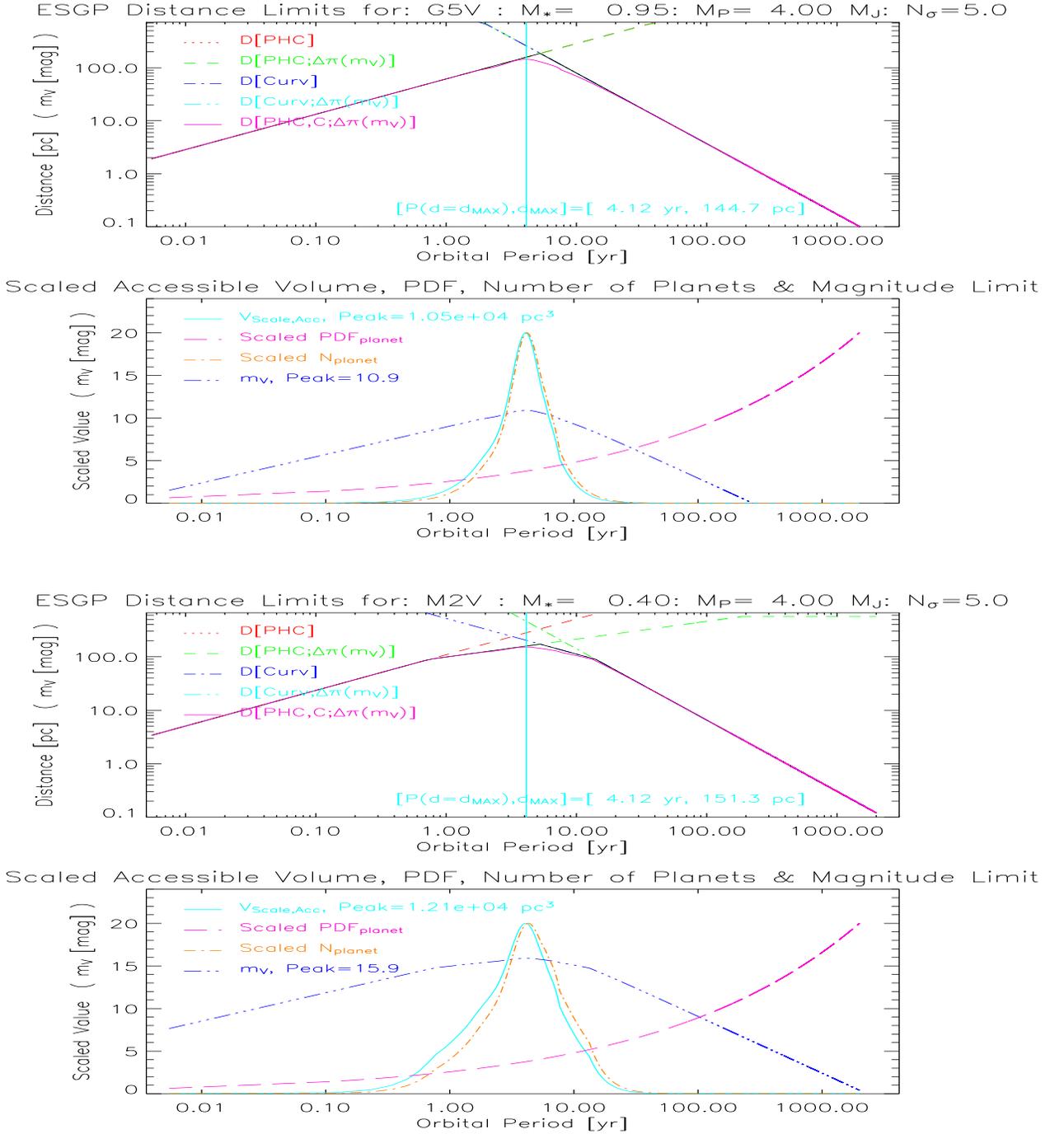
Fig. 2.— These plots show the analyses for a G5V primary (top plot) and a M2V star (bottom panel). For a full explanation of the figures, see figure 1. Both figures are for OBSS-A/GAIA mission parameters.

$P_1 \leq P \leq P_2$. The bottom panels of figures 1 and 2 clearly show that the PDF (dashed, purple line) rises towards longer periods. (This plotted PDF is integrated over $\pm 1\%$ of the period plotted on the abscissa and $\pm 1\%$ of the mass listed in the figure's title). In fact, the PDFs of eqn. (30) is not bound: extending the integration boundaries to infinity yields an infinite probability, and is hence unphysical. However, such extensions to infinity are unphysical as well, so that eqns. (30) and (31) summarize the current state of affairs to reasonable accuracy. In the remainder of the memo, I assume that this PDF is independent of the spectral type (mass) of the primary.

3.3. Number of ESGPs

The number of expected extra-solar giant planets is the integral over the PDF and the number of stars, and is a function ($\mathcal{F}$) of properties of the stellar primary $[M_V, \rho_*(M_V), h_z(M_V)]$, mission parameters $[T_M, V_f(M_V), \delta_{X0,f}]$, and the required accuracy $[N_\sigma]$:

$$N_{ESGP} = \mathcal{F}(M_V, \rho_*(M_V), h_z(M_V), T_M, V_f(M_V), \delta_{X0,f}, N_\sigma) \tag{32}$$

$$N_{ESGP} = \rho_*(M_V) \int_{P=2\,days}^{P=900\,years} dP \int_{M=0.1\,M_J}^{M=12\,M_J} dM \times$$
$$Prob_{PL}(P, M) \times Vol(P, M; M_V, h_z(M_V), T_M, V_f(M_V), \delta_{X0,f}, N_\sigma) \; , \tag{33}$$

where $\rho_*(M_V)$ and $h_z(M_V)$ are the type-dependent stellar density and scaleheight of the population, and $V_f(M_V)$ the type-dependent floor magnitude[3]. I solve eqn. (33) on a fine grid in P (3,000 cells) and M (300 cells), where I assume that the volume is constant in a cell and evaluate it at the center of the cell. Integrating eqn. (33) over a cell then reduces to multiplying this volume by the integral of the PDF over the cell [using eqn. (31)]. The total number of ESGPs then simply equals the sum over all grid points.

The expected number of ESGPs (dashed-dotted, orange line in figures 1 and 2 depends strongly upon orbital period. In fact, the curve is rather strongly peaked, indicating that most detections will be made in a fairly small range of periods, and hence distances and magnitudes. For the particular case plotted in figure 1, the full-width at quarter maximum (FWQM) range corresponds to periods ranging from 1.9 to 9.1 years and a magnitude interval from 7.6 to 9.0, and a distance range of 140 to 264 pc. For *orbit determination* with a three times larger signal-to-noise requirement, the range in orbital periods is just slightly smaller,

---

[3]For AV, FV, G5, KV and MV stars, I use the following values for V_f, (ρ_*) and $[h_z]$: 14.0, 14.10, 14.20, 14.44 and 14.75 mag (0.938, 4.70, 11.79, 18.76, 63.50 stars per 1000 pc^3) [100, 200, 280, 300, 300 pc]. As stellar masses I use: 2.00, 1.26, 0.95, 0.63, and 0.40 $M_\odot$. See also table 5

but the primaries are roughly three times closer, and the stars 2.4 mag brighter at $V \sim 5.9$. Also note that the less massive planets are possibly more interesting to study: the parent star of a 1 Jupiter-mass planet needs to be 12 times closer and will hence be 5.4 mag brighter at $V \sim 2.9$ for "detection" and at $V \sim 0.5$ for orbit determination. Similar plots are shown for a G5V and M2V primary and a 4 Jupiter-mass planets in figure 2.

A summary of the dependence of the properties on planet masses is presented in tables 1 and 2 for OBSS-A and in tables 3 and 4 for OBSS-B. Graphically, the results for OBSS-A are presented in figures 3 and 4, where the scales are linear and logarithmic, respectively[4]. The same data for OBSS-B mission parameters is presented in figures 3 and 4. The structure of these figures is the same: the left-hand column is for detections, the right-hand column for orbit determinations. Each sub-panel corresponds to a particular spectral type. In each of the panels, the thick horizontal line (black) gives the period [$\sim 0.82 T_M$, cf., eqn. (22)] that corresponds to the maximum distance out to which a particular star-planet can be recognized. The dotted lines (black) are the orbital periods where the ESGP number count has dropped to one-quarter of the peak. The dashed-dotted lines gives the number of ESGPs for integrated over all periods and a 1% range in planetary mass, where all curves in a column are scaled by the same maximum. As can be seen from the dashed and dashed-dotted lines (red) of figure 3, the magnitude-range corresponding to $FWQM$ and the faintest magnitude is quite small, typically about 1.2 magnitudes. This is the result of the small distance range ($\pm 13\%$) over which most ESGPs of a given mass will be recognized. [The (purple) dashed-triple-dotted lines are the corresponding distance limits (in figure 4)].

The magnitude and distance ranges presented here are only valid for the particular spectral subtype used. The actual ranges for a given spectral type will be larger because there is intrinsic spread in the absolute magnitude for stars of a given mass (due to the age spread), and because the stellar masses and luminosities change with spectral type.

4. Mission Design Considerations

Several qualitative conclusions can be drawn from the work presented above with regard to planet detection (PD) and orbit determination (OD). For more details, see tables 1 through 4.

- The largest number of ESGPs will be found with periods close to 0.82 times the mission

---

[4]Note that these results are obtained for the OBSS-A configuration, but are valid for all missions that have a mission duration of 5 years and a astrometric accuracy of 10μas.

Table 1.   Expected number of "Detected" ESGPs
for OBSS-A/GAIA mission parameters.

		Planet Detection: $N_\sigma = 5$					
$M_{PL} \rightarrow$	0.5	1.0	2.0	4.0	8.0	12.0	TOT
SPT↓	Number of Planets						
A5V	0	0	0	3	16	34	53
F5V	0	1	5	35	224	496	761
G5V	0	3	22	155	1,020	2,295	3,495
K5V	2	11	79	544	3,188	4,838	8,662
M2V	15	92	592	2,113	5,730	6,796	15,338
TOT	17	107	698	2,850	10,178	14,459	28,309
$M_{PL} \rightarrow$	0.5	1.0	2.0	4.0	8.0	12.0	
SPT↓	V-magnitude						
A5V	1.5	3.1	4.5	6.0	7.5	8.3	
F5V	3.8	5.3	6.8	8.3	9.8	10.6	
G5V	5.8	7.3	8.8	10.3	11.8	12.6	
K5V	8.7	10.2	11.7	13.2	14.2	14.6	
M2V	12.0	13.5	14.6	15.3	16.0	16.4	
$M_{PL} \rightarrow$	0.5	1.0	2.0	4.0	8.0	12.0	
SPT↓	Distance [pc]						
A5V	9	18	35	69	137	202	
F5V	12	24	48	95	187	276	
G5V	14	29	57	114	226	334	
K5V	19	38	75	150	242	292	
M2V	26	51	84	117	164	200	

Note. — Number of *detected planets* (top part of the table), magnitude requirements (middle part) and maximal distances (bottom part) for planet detection ($N_\sigma = 5$) for missions with GAIA and/or OBSS-A parameters. The columns correspond to different planet mass ranges. The first column integrates over 0.1 to 0.5 M_J, and the ith column integrates over the mass listed in column $i - 1$ to the mass of column i.

Table 2. Expected number of ESGPs with determined orbits
for OBSS-A/GAIA mission parameters.

		Planet Detection: $N_\sigma = 15$					
$M_{PL} \rightarrow$	0.5	1.0	2.0	4.0	8.0	12.0	TOT
SPT↓	Number of Planets						
A5V	0	0	0	0	1	2	3
F5V	0	0	0	1	10	24	35
G5V	0	0	1	6	44	107	158
K5V	0	0	3	22	155	373	553
M2V	1	4	26	182	936	1,307	2,456
TOT	1	4	30	211	1,146	1,813	3,205
$M_{PL} \rightarrow$	0.5	1.0	2.0	4.0	8.0	12.0	
SPT↓	V-magnitude						
A5V	-0.8	0.7	2.2	3.7	5.1	6.0	
F5V	1.4	2.9	4.4	5.9	7.4	8.3	
G5V	3.4	4.9	6.4	7.9	9.4	10.3	
K5V	6.3	7.8	9.3	10.8	12.3	13.2	
M2V	9.6	11.1	12.6	14.1	14.8	15.2	
$M_{PL} \rightarrow$	0.5	1.0	2.0	4.0	8.0	12.0	
SPT↓	Distance [pc]						
A5V	3	6	12	23	46	69	
F5V	4	8	16	32	63	94	
G5V	5	10	19	38	76	114	
K5V	6	13	25	50	100	149	
M2V	9	17	34	68	96	117	

Note. — For an explanation of the columns, see table 1.

Table 3.   Expected number of "Detected" ESGPs
for OBSS-B mission parameters.

	Planet Detection: $N_\sigma = 5$						
$M_{PL} \rightarrow$	0.5	1.0	2.0	4.0	8.0	12.0	TOT
SPT↓	Number of Planets						
A5V	0	0	0	0	2	4	6
F5V	0	0	0	3	24	58	85
G5V	0	0	2	16	108	260	386
K5V	0	1	8	55	380	897	1,341
M2V	1	9	64	431	1,652	2,128	4,285
TOT	1	10	74	505	2,166	3,347	6,103
$M_{PL} \rightarrow$	0.5	1.0	2.0	4.0	8.0	12.0	
SPT↓	V-magnitude						
A5V	-0.2	1.3	2.8	4.3	5.8	6.7	
F5V	2.1	3.6	5.1	6.6	8.1	9.0	
G5V	4.1	5.6	7.1	8.6	10.1	11.0	
K5V	7.0	8.5	10.0	11.5	13.0	13.8	
M2V	10.3	11.8	13.3	14.4	15.1	15.6	
$M_{PL} \rightarrow$	0.5	1.0	2.0	4.0	8.0	12.0	
SPT↓	Distance [pc]						
A5V	4	8	16	32	63	94	
F5V	5	11	22	43	86	128	
G5V	7	13	26	52	103	155	
K5V	9	17	34	68	136	202	
M2V	12	23	47	80	112	136	

Note. — Number of *detected planets* (top part of table), magnitude requirements (middle) and maximal distances (bottom) for planet detection ($N_\sigma = 5$) for missions with OBSS-B parameters ($\delta_{X0,f} = 22$ μas). The columns correspond to different planet mass ranges. The first column integrates over 0.1 to 0.5 M_J, and the ith column integrates over the mass listed in column $i - 1$ to the mass of column i.

Table 4.   Expected number of ESGPs with determined orbits
for OBSS-B mission parameters.

	Orbit Determination: $N_\sigma = 15$						
$M_{PL} \rightarrow$	0.5	1.0	2.0	4.0	8.0	12.0	TOT
SPT↓	Number of Planets						
A5V	0	0	0	0	0	0	0
F5V	0	0	0	0	1	2	3
G5V	0	0	0	1	4	11	16
K5V	0	0	0	2	15	38	55
M2V	0	0	2	18	126	291	437
TOT	0	0	2	21	146	342	511
$M_{PL} \rightarrow$	0.5	1.0	2.0	4.0	8.0	12.0	
SPT↓	V-magnitude						
A5V	-2.6	-1.0	0.5	2.0	3.5	4.3	
F5V	-0.3	1.2	2.7	4.2	5.7	6.6	
G5V	1.7	3.2	4.7	6.2	7.7	8.6	
K5V	4.6	6.1	7.6	9.1	10.6	11.5	
M2V	7.9	9.4	10.9	12.4	13.9	14.4	
$M_{PL} \rightarrow$	0.5	1.0	2.0	4.0	8.0	12.0	
SPT↓	Distance [pc]						
A5V	1	3	5	11	21	32	
F5V	2	4	7	14	29	43	
G5V	2	4	9	17	35	52	
K5V	3	6	11	23	46	68	
M2V	4	8	16	31	61	80	

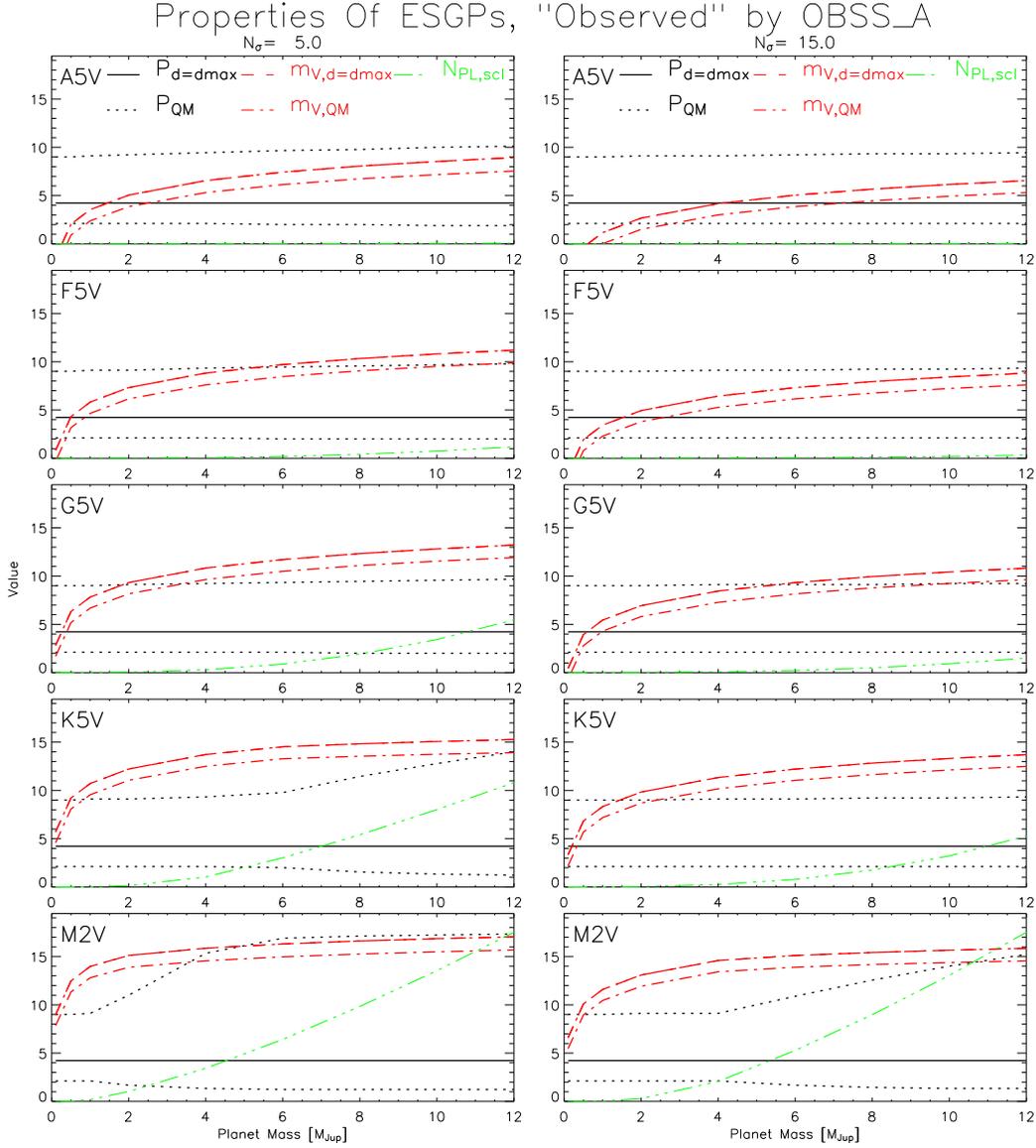Note. — For an explanation of the columns, see table 3.

Fig. 3.— Summary of properties of ESGPs as "observed" by OBSS-A/GAIA for 5 spectral types: A5V, F5V, G5V, K5V and M2V from top to bottom. Results for "detections" (5σ) are presented in the left column, and for "orbit determination" (15σ) in the right-hand column. The thick drawn (black) lines represent the period where maximal distance (volume) is achieved. The dotted lines (black) are the periods where the number of ESGPs [$N_{ESGP}(P)$] has dropped to $N_{ESGP}(P) = \frac{1}{4}N_{ESGP}^{MAX}$. The dashed and dashed-dotted lines (red) are the magnitudes that correspond to the peak of the same points on the $N_{ESGP}(P)$ curve. The dashed-triple-dotted line (green) corresponds to the (scaled) number of detectable ESGPs. The number of expected ESGPs is scaled separately for the two columns.
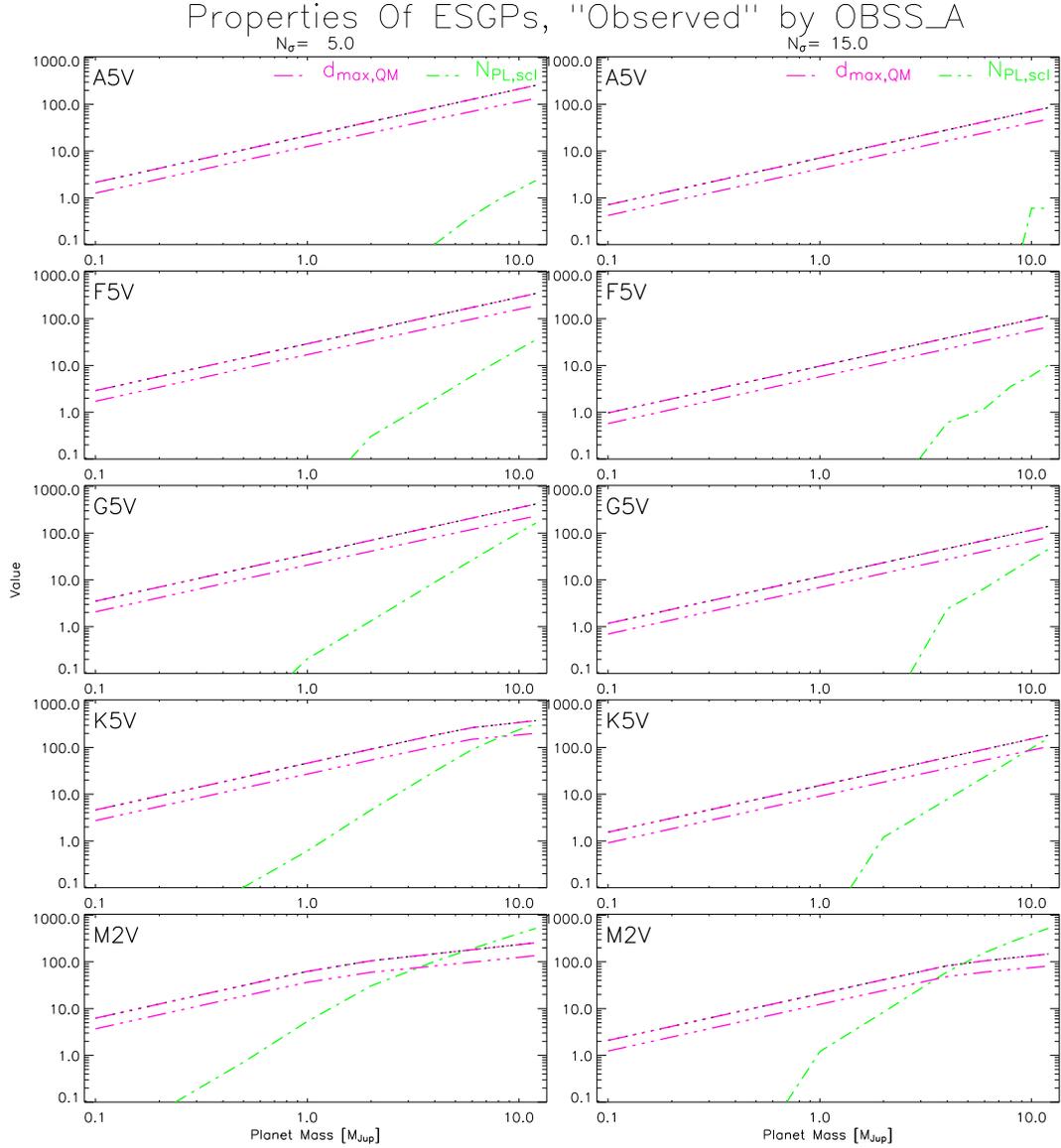
Fig. 4.— Summary of properties of ESGPs as "observed" by OBSS-A/GAIA for 5 spectral types: A5V, F5V, G5V, K5V and M2V from top to bottom. Results for "detections" and "orbit determinations" are plotted in the left- and the right-hand columns, respectively. The dashed-triple-dotted lines (magenta) are the distances where $N_{ESGP}(P) = N_{ESGP}^{MAX}$ and $N_{ESGP}(P) = \frac{1}{4}N_{ESGP}^{MAX}$. As in figure 3, the dashed-triple-dotted line (green) corresponds to the (scaled) number of detectable ESGPs, with different scaling for the two columns.
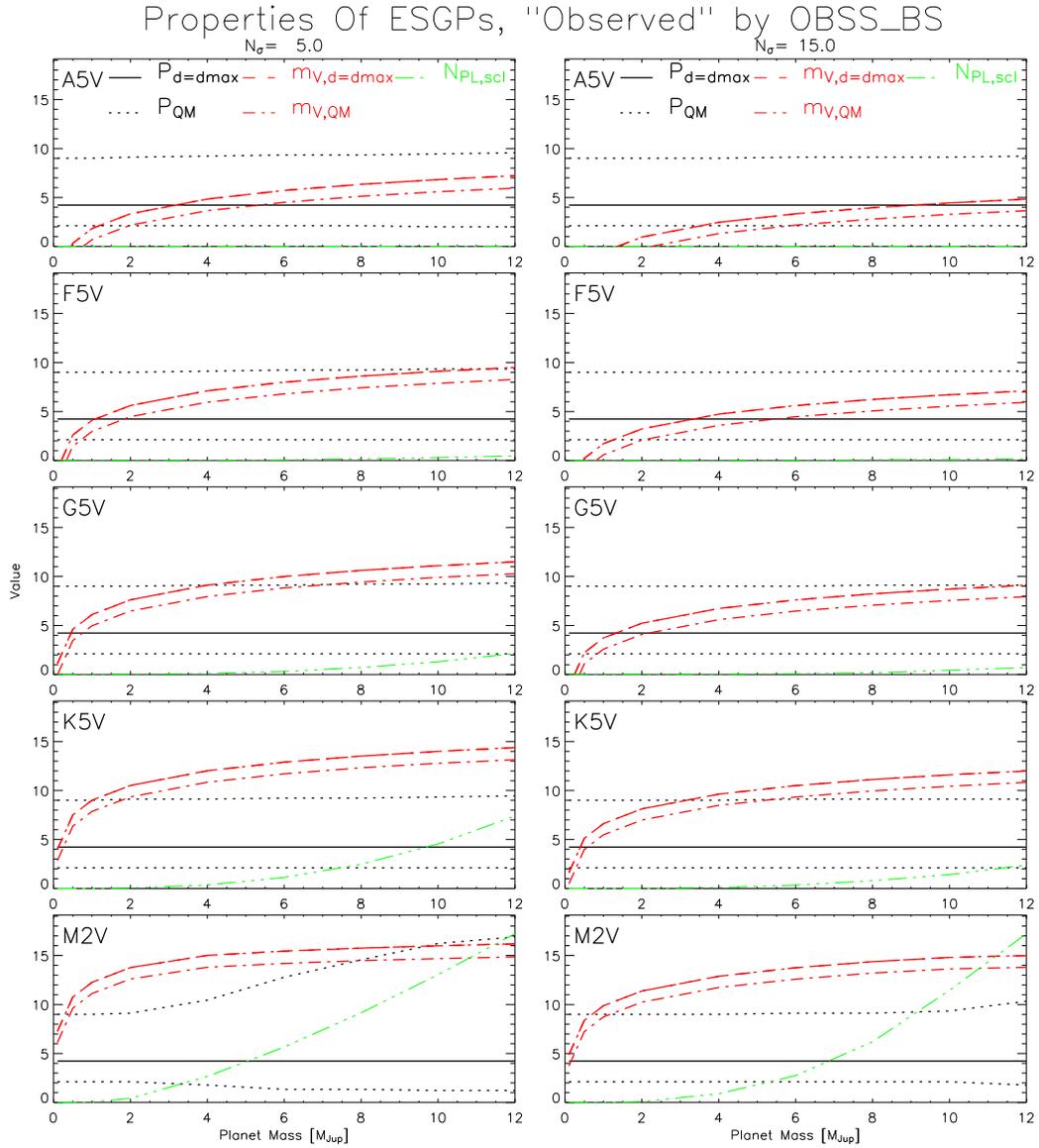
Fig. 5.— Summary of properties of ESGPs as "observed" by OBSS-B. For a full explanation of the plots, see figure 3.
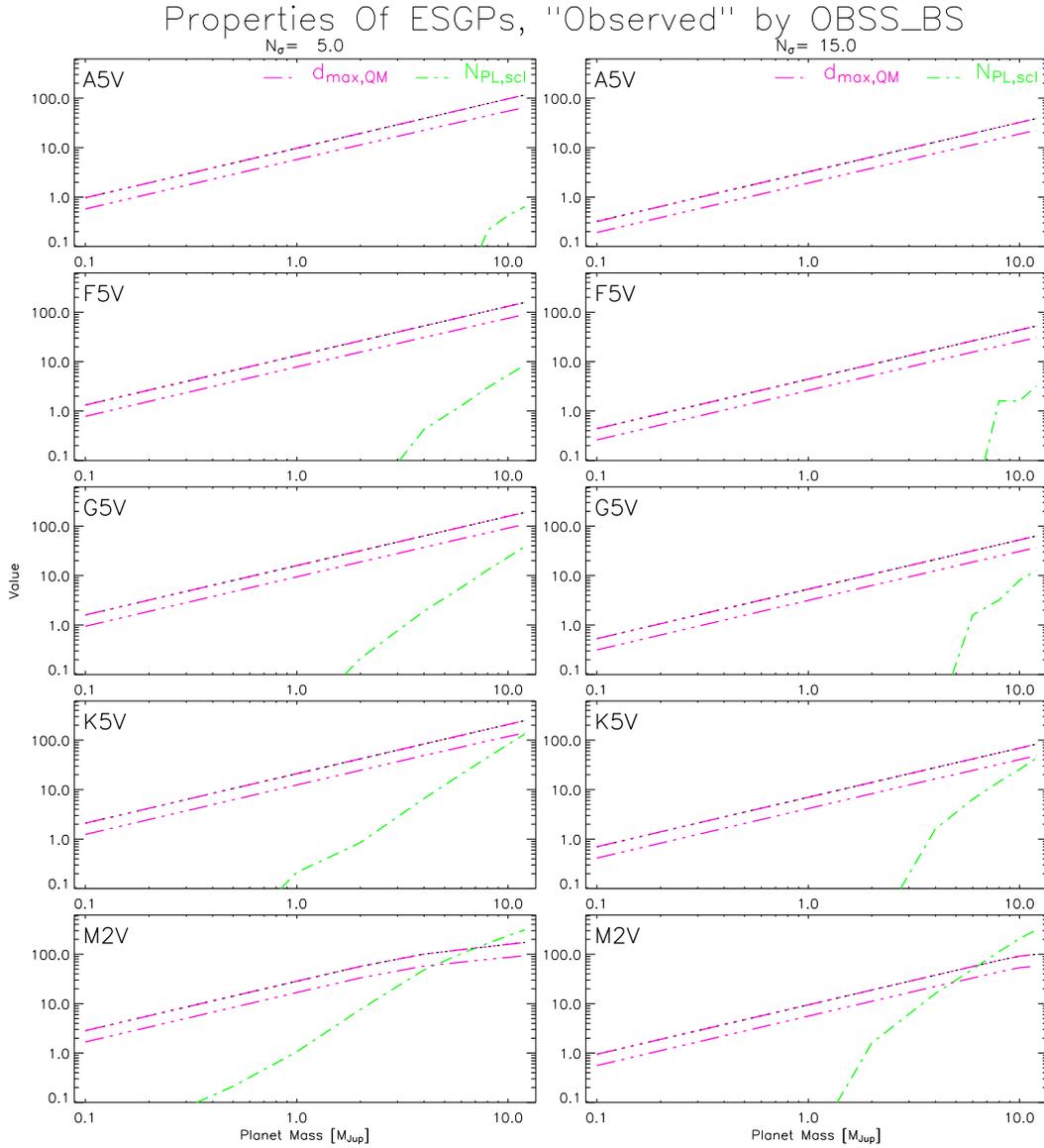
Fig. 6.— Summary of properties of ESGPs as "observed" by OBSS-B. For a full explanation of the plots, see figure 4.

duration (4.12 years for OBSS/GAIA).

- For A stars, the period range is roughly 2 to 10 years, for M stars the range is 1 to 15 years.

- If a sample is complete to a given distance for a certain planetary mass, then the sample will also be complete for all larger planetary masses

- Most ESGPs of a given mass will be detected in a small range of period, distance & apparent magnitude. For example, for a planets in the range of 4 to 6 M_J, I get:

  - The full magnitude range for PDs [ODs] for G-type stars is 10.6 to 11.8 [8.2 to 9.4] for OBSS-A and 8.9 to 10.1 [6.6 to 7.7] for OBSS-B.

  - The corresponding distance ranges are 124 to 217 pc [42 to 72 pc] for OBSS-A and 58 to 99 pc [19 to 33 pc] for OBSS-B.

- Most PDs and ODs are found among M-type stars

- The fraction of M star with PDs and ODs *increases* as the astrometric accuracy decreases and/or the detection threshold increases. For example,

  - The fraction of PDs [ODs] for M-type stars increases from 54% [77%] for OBSS-A to 70% [86%] for OBSS-B.

- The fraction of "interesting" ESGPs *declines* strongly as the astrometric accuracy decreases and/or the detection threshold increases. For example,

  - The fraction of PDs [ODs] for G-type stars declines from 12.3% [4.9%] for OBSS-A to 6.3% [3.1%] for OBSS-B.

  - The number of PDs [ODs] with masses between 2 and 4 M_J for G-type stars declines from 155 [6] for OBSS-A to 16 [1] for OBSS-B.

More specifically, if we use the number of detectable planets as a metric for the success of the mission, it is possible to estimate how this number varies with mission parameters. As a first step, the expected number scale with the accessible volume, which is approximated as $V \sim \pi h_z^3 (\frac{d_{lim}}{h_z})^\kappa$ [see eqn. (27)]. Unfortunately, the derivation of d_{lim} is fairly involved. I will go through the steps sequentially and present the results in tabular form in tables 5 and 6.

1. Determine the transition distance

   (a) Determine the floor magnitude (V_f), which is spectral type dependent

(b) Determine the absolute magnitude of the stars

(c) $d_{tr}(M_V, V_f) = 10^{[V_f(M_V)+5-M_V]/5}$

2. Determine the distance that corresponds to the faintest allowable magnitude $[V_{f+}(M_V)]$

   (a) $d_{f+}(M_V, V_f) = 10^{(V_{f+}+5-M_V)/5}$, where I use $V_{f+} = V_f + 4$, so that

   (b) $d_{f+} \sim 6.3\, d_{tr}$.

3. Determine d_{max} according to eqn. (23).

4. Determine d_{lim}, which depends on:
   I) mission duration, II) stellar mass, III) planetary mass, IV) the floor for the astrometric accuracy, and V) the detection threshold

   (a) IF $d_{max} \leq d_{tr}$ THEN $d_{lim} = d_{max}$

   (b) ELSE $d_{lim} = \sqrt{d_{max}\, d_{tr}}$, according to eqn. (24).

   (c) IF $d_{lim} \geq d_{f+}$ THEN $d_{lim} = d_{f+}$

5. The number of ESGPs is proportional to:
   $N_{ESGP} = Prob_{PL,ave}\, \rho_*\, V(d_{max}) \approx Prob_{ave}\, \pi\, \rho_*\, h_z^3\, (d_{max}/h_z)^\kappa$, where $\kappa \sim 2.7$ with a slight variation depending on the value of (d_{max}/h_z).

   (a) The actual number of expected ESGPs *for a given spectral type* is predicted accurately (to $\pm$ 10%) when using $Prob_{PL,ave} = 0.01$, and the d_{max} value appropriate for that spectral type.

   (b) $Prob_{PL,ave}$ depends on the mission duration because the mission duration determines which part of the PDF will be best sampled.

6. Scaling the number of ESGPs as a function of mission accuracy goes as follows:

   (a) IF 4(a), THEN $d_{max} \propto 1/\delta_{X0,f}$ and $N_{ESGP} \propto (1/\delta_{X0,f})^\kappa$

   (b) IF 4(b), THEN $d_{max} \propto \sqrt{1/\delta_{X0,f}}$ and $N_{ESGP} \propto (1/\delta_{X0,f})^{\kappa/2}$

   (c) IF 4(c), THEN d_{max} is independent of $\delta_{X0,f}$

When only a small range in planetary masses and periods is considered, equation (33) simplifies considerably because the integral $Prob_{PL}$ over P and M can be considered constant. In that case, the relative number of ESGPs between case "A" and "B" are easily calculated:

$$\frac{N_{ESGP}^A}{N_{ESGP}^B} \sim \frac{\rho_{*A}}{\rho_{*B}} \times \frac{Vol(d_{max,A})}{Vol(d_{max,B})} \times \frac{Prob_{PL}(A)}{Prob_{PL}(B)} \tag{34}$$

where the volumes are determined via eqn. (27) and d_{max} from eqns. (23) and (24). In the general case, one can use eqn. (31) to approximate the ratio of the probabilities. For the specific case of determining the relative numbers detected by OBSS-A versus OBSS-B, the only difference between case A & B is the astrometric accuracy. Still, for this simple problem three solutions exist depending on the relative location of d_{max} with respect to the transition distance: I) both distances are smaller than d_{tr}, the d_{max} ratio equals $\tilde{d}_{max,A}/\tilde{d}_{max,B} = 22/10 = 2.2$, II) both distances are larger than d_{tr}, so that $\tilde{d}_{max,A}/\tilde{d}_{max,B} = \sqrt{22/10} = 1.5$, III) case A exceeds d_{tr} and case B does not, the distance ratio equals $\sqrt{22/10}\,\sqrt{d_{tr}/d_{max,B}}$. The first two solutions only depend on the ratio of the astrometric accuracies, while for the third solution the parameters of the binary system come in via the second square-root term.

Based on conditions 6(a) and 6(b) and eqn. (34) above, I expect that scaling from OBSS-A/GAIA to OBSS-B yields $2.2^{2.7} \sim 8.4$ times fewer ESGPs for those primaries that have $d_{max} < d_{tr}$ and $1.5^{2.7} = 3$ times fewer ESGPs when $d_{max} > d_{tr}$ [with $\kappa{=}2.7$]. Obviously, since the ratios are so different on the two sides of d_{tr}, the scaling will be less accurate close to the transition distance, especially when the distances for the two missions bracket the transition distance. Generally speaking, the scaling procedure outlined above works to within $\pm20\%$ or so. For the case of OBSS-A to OBSS-B scaling 10 to 30% occur when the limiting distance is on the same side of the transition distance. However, errors of order 80% occur when the limiting distances of the two missions lie on either side of d_{tr}. For the total number of ESGPs, this scaling *over*estimates the number of ESGPs by roughly 50%. Note that the scaling procedure [1(a) through 6(c)] is, strictly speaking, valid for just a single planetary mass. Nevertheless, by picking a mass somewhere in the middle (5.25 M_J), the scaling is accurate to about 30%.

If one wants to use a single metric to quantify the mission's performance I would recommend to use MV stars because only for these stars the limiting distance is almost always larger than the transition distance, and because the majority of ESGPs will be found around M-type stars. In that case, equation (34) can be applied to predict the relative performance of the missions. However, the drawback of this metric is that it is hard to predict the number of "interesting" ESGPs, such as the number of planets around early-type stars or the number of low-mass planets around G-type stars.

5. Conclusion

The number of ESGPs detected (5σ) with a configuration like OBSS-A/GAIA are tabulated in table 1 and the number of ESGPs for which orbits might be determined in table 2. The OBSS-B results are summarized in tables 3 and 4. The numbers for OBSS-A are substantially smaller than previously reported. For the stellar types in common, this work reports *de*creases by about a factor of 10 for ODs and a factor of 2 for PDs. These differ-

Table 5.   Mission Scaling Relation Worksheet for OBSS-A and GAIA.

	A5V	F5V	G5V	K5V	M2V	Comments
ρ_* [stars/1000 pc^3]	0.938	4.70	11.79	18.76	63.50	
h_z [pc]	100	200	280	300	300	
M_V [mag]	1.90	3.50	5.10	7.40	10.00	
M_* [$M_\odot$]	2.00	1.26	0.95	0.63	0.40	
V_f [mag]	14.00	14.10	14.20	14.44	14.75	
d_{tr} [pc]	2,630	1,318	661	256	89	eqn. (12)
d_{f+} [pc]	16,595	8,317	4,168	1,614	562	eqn. (13)
	$M_{PL} = 5.25\,M_J, N_\sigma{=}5$ and $d_{X0,f} = 10\,\mu$as					
d_{max} [pc]	123	167	202	265	357	eqn. (23)
$d_{max} < d_{tr}$?	yes	yes	yes	no	no	
$d_{lim,1}$ [pc]	123	167	202	260	178	
$d_{lim} > d_{f+}$?	no	no	no	no	no	
d_{lim} [pc]	123	167	202	260	178	
d_{lim}/h_z	1.23	0.84	0.72	0.87	0.59	
κ	2.61	2.67	2.70	2.67	2.72	eqn. (28)
Vol_{acc} [10^6 pc^3]	5.4	15.6	28.5	58.0	20.6	eqn. (27)
$N^{scl}_{ESGP,ANA}(M_{PL} = 5.25)$	1.0	14.5	66.4	215.4	258.6	eqn. (34)
$N^{scl}_{ESGP,NUM}(all\ M_{PL})$	1.0	14.7	67.3	170.9	305.5	
$N^{scl}_{ESGP,ANA}/N^{scl}_{ESGP,NUM}$	1.00	0.99	0.99	1.26	0.85	
	$M_{PL} = 5.25\,M_J, N_\sigma{=}15$ and $d_{X0,f} = 10\,\mu$as					
d_{max} [pc]	41	56	67	88	119	
$d_{max} < d_{tr}$?	yes	yes	yes	yes	no	
$d_{lim,1}$ [pc]	41	56	67	88	103	
$d_{lim} > d_{f+}$?	no	no	no	no	no	
d_{lim} [pc]	41	56	67	88	103	
d_{lim}/h_z	0.41	0.28	0.24	0.29	0.34	
κ	2.78	2.82	2.84	2.82	2.80	
Vol_{acc} [10^6 pc^3]	0.3	0.7	1.2	2.7	4.3	
$N^{scl}_{ESGP,ANA}(M_{PL} = 5.25)$	1.0	12.9	57.0	204.1	1090.3	
$N^{scl}_{ESGP,NUM}(all\ M_{PL})$	1.0	11.0	50.7	177.0	808.3	
$N^{scl}_{ESGP,ANA}/N^{scl}_{ESGP,NUM}$	1.00	1.17	1.13	1.15	1.35	

Note. — The top part of the table lists parameters that are intrinsic to the stars, for five different spectral types (the columns). The middle and bottom parts of the table follows the decision tree enumerated in section 4 as steps 1(a) through 6(c). The middle part is for planet detection (5 σ), and the bottom part for orbit determination (15 σ). The last three lines of the middle and bottom parts give: 2) the expected ration of ESGPs according to the "worksheet," normalized to unity for A5 stars, 2) the actual number of ESGPs according to the full numerical integration (also normalized to the A5V count), and 3) the ratio of the the two.

Table 6.   Mission Scaling Relations: OBSS-B and OBSS-A to OBSS-B.

	A5V	F5V	G5V	K5V	M2V	TOT
	$M_{PL} = 5.25\,M_J, N_\sigma{=}5$ and $d_{X0,f} = 22\ \mu$as					
d_{max} [pc]	56	76	92	120	162	
$d_{max} < d_{tr}$?	yes	yes	yes	yes	no	
$d_{lim,1}$ [pc]	56	76	92	120	120	
$d_{lim} > d_{f+}$?	no	no	no	no	no	
d_{lim} [pc]	56	76	92	120	120	
d_{lim}/h_z	0.56	0.38	0.33	0.40	0.40	
κ	2.73	2.79	2.81	2.78	2.78	
Vol_{acc} [10^6 pc^3]	0.6	1.7	3.0	6.7	6.7	
$N^{scl}_{ESGP,ANA}(M_{PL} = 5.25)$	1.0	13.2	59.0	208.7	706.3	
$N^{scl}_{ESGP,NUM}(all\ M_{PL})$	1.0	13.5	61.7	214.7	708.2	
$N_{ESGP,ANA}/N_{ESGP,NUM}$	1.00	0.98	0.96	0.97	1.00	
$N_{ESGP,OBSS-A2B}/N_{ESGP,OBSS-B}$	0.86	0.93	1.60	1.65	1.15	1.28
	$M_{PL} = 5.25\,M_J, N_\sigma{=}15$ and $d_{X0,f} = 22\ \mu$as					
d_{max} [pc]	19	25	31	40	54	
$d_{max} < d_{tr}$?	yes	yes	yes	yes	yes	
$d_{lim,1}$ [pc]	19	25	31	40	54	
$d_{lim} > d_{f+}$?	no	no	no	no	no	
d_{lim} [pc]	19	25	31	40	54	
d_{lim}/h_z	0.19	0.13	0.11	0.13	0.18	
κ	2.86	2.89	2.90	2.89	2.87	
Vol_{acc} [10^6 pc^3]	0.03	0.06	0.11	0.25	0.63	
$N^{scl}_{ESGP,ANA}(M_{PL} = 5.25)$	1.0	12.5	54.9	198.2	1657	
$N^{scl}_{ESGP,NUM}(all\ M_{PL})$	1.0	11.7	58.4	206.2	1642	
$N_{ESGP,ANA}/N_{ESGP,NUM}$	1.00	1.07	0.94	0.96	1.01	
$N_{ESGP,OBSS-A2B}/N_{ESGP,OBSS-B}$	1.20	1.13	1.04	1.76	1.84	1.81

Note. — Table layout is similar to that of table 5, except that the rows specifying the stars intrinsic to the star are omitted. Furthermore, I have added one row to each of the two parts of the table. The last row indicates the ratio of the expected number of OBSS-B ESGPs based on scaling the OBSS-A results and the actual OBSS-B results.

ences are due several improvements of the procedure: I) Here I use a self-consistent criterion for the photocenter- and the curvature distances that is tailored to "binary" systems with periods roughly equal to the mission period, II) I have extended the analysis beyond V_f, and III) for this memo, the calculations are done on a much finer grid. The first improvement is responsible for most of the differences.

Scaling relations developed in section 4 can be used to calculate the relative numbers of ESGPs as a function of spectral type, orbital period or planetary mass [eqn. (34). The following general conclusions hold, independent of mission architecture: I) the majority (54% to 86%) of ESGPs is expected to be found around M-type stars, II) the number of "interesting" ESGPs (low-mass planets and/or high-mass primaries) is roughly three times more sensitive to changes in mission parameters than the overall number of ESGPs, III) most of the uncovered ESGPs have a small range of orbital periods ($\frac{1}{2}$ to twice the mission duration), IV) for a given binary, most of the ESGPs will be found around primaries with a small magnitude range (±0.7 mag), V) the masses of the uncovered ESGPs will tend to be large, VI) "interesting" systems will have bright primaries.

Comparing the specific case of OBSS-A/GAIA versus OBSS-B, I find the following:

1. OBSS-A/GAIA will detect 28,300 ESGPs, versus 6,100 (4.6 times fewer) for OBSS-B

2. OBSS-A/GAIA will be able to determine orbits for 3,200 systems, versus 510 for (6.3 times fewer) for OBSS-B

3. OBSS-A/GAIA [OBSS-B] can detect 17 [1] ESGPs with masses below 0.5 M_J. The magnitudes of these systems are between 8.7 and 12.0 [7.0 to 10.3].

4. OBSS-A/GAIA [OBSS-B] can determine orbits for 30 [2] ESGPs with masses below 2 M_J. The magnitudes of these systems are between 9.3 and 12.6 [9.6 to 10.9].

5. For G-type stars, OBSS-A/GAIA [OBSS-B] will be able to detect 3,500 [390, or 9 times fewer] ESGPs. The magnitudes of these systems are between 7.3 and 12.6 [7.1 to 11.0].

6. For G-type stars, OBSS-A/GAIA [OBSS-B] will be able to determine orbits for 158 [16, or 10 times fewer] ESGPs. The magnitudes of these systems are between 6.4 and 10.3 [6.2 to 8.6].

7. et. cetera.

To summarize, an OBSS-A/GAIA type mission will discover many ESGPs, over a wide range of spectral types, and planetary masses. OBSS-B, with twice worse accuracy will

still discover several thousand ESGPs but can determine orbits for just a couple of hundred systems. For "interesting" planets, the penalty incurred from poorer astrometric accuracy is substantially larger than for the majority of the ESGPs. For both missions, the parent stars of the ESGPs will have magnitudes brighter than $V = 16$ [$V = 13$] for detection [orbit determination]. In the game of astrometric planet detection, there is no substitute for astrometric accuracy.